Substantial Influence of ERAP2 on the HLA-B*40:02 Peptidome: Implications for HLA-B*27-Negative Ankylosing Spondylitis

Authors

Elena Lorente, Jennifer Redondo-Antón, Adrian Martín-Esteban, Pablo Guasp, Eilon Barnea, Pilar Lauzurica, Arie Admon, and José A. López de Castro

Correspondence

elorente@isciii.es

In Brief

ERAP2 and HLA-B*40:02 are associated with ankylosing spondylitis independently of HLA-B*27. ERAP2 process MHC-I ligands, preferentially trimming N-terminal basic residues. The B*40:02 peptidomes from wild-type and ERAP2-KO cells were compared, which demonstrated a substantial role of ERAP2 on the generation/destruction balance of HLA-B*40:02 ligands. The major effect was on N-terminal residues, although other peptide positions were also affected. We propose that the non-epistatic association of ERAP2 with spondyloarthropathy might be related to processing of peptides with N-terminal basic residues.

Graphical Abstract

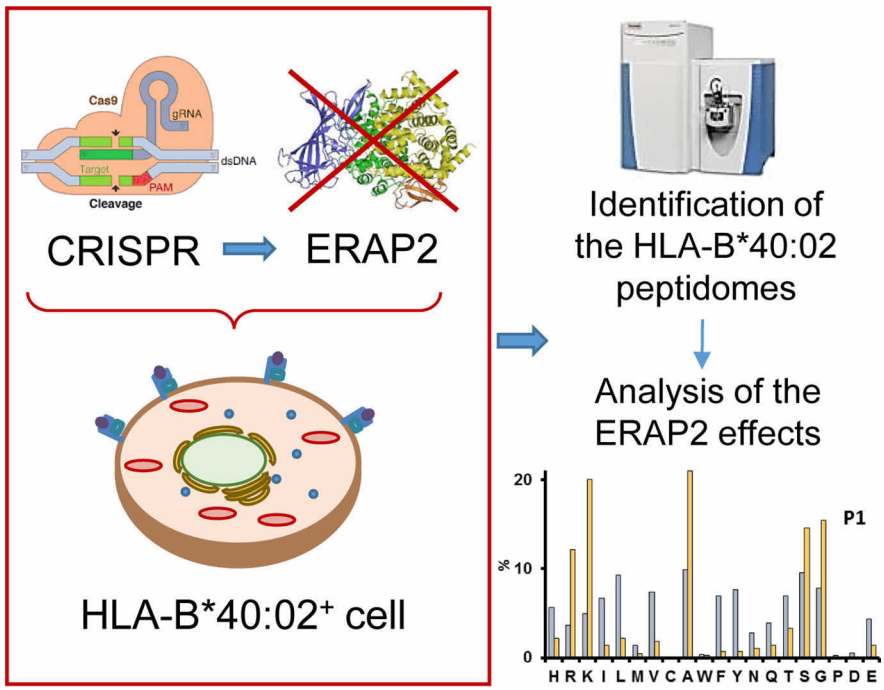

Highlights

- HLA-B*40:02 and ERAP2 are risk factors for ankylosing spondylitis.
- The effects of ERAP2 on the B*40:02 peptidome are defined.
- ERAP2 has a major influence mainly due to alterations of N-terminal residues.
- These effects provide a basis for the association of ERAP2 with disease.

Lorente et al., 2019, Molecular & Cellular Proteomics *18*, 2298–2309

https://doi.org/10.1074/mcp.RA119.001710

Substantial Influence of ERAP2 on the HLA-B*40:02 Peptidome: Implications for HLA-B*27-Negative Ankylosing Spondylitis*[S]

Elena Lorente‡§‖, Jennifer Redondo-Antón§, Adrian Martín-Esteban‡, Pablo Guasp‡, Eilon Barnea¶, Pilar Lauzurica§, Arie Admon¶, and José A. López de Castro‡

HLA-B*40:02 is one of a few major histocompatibility complex class I (MHC-I) molecules associated with ankylosing spondylitis (AS) independently of HLA-B*27. The endoplasmic reticulum aminopeptidase 2 (ERAP2), an enzyme that process MHC-I ligands and preferentially trims N-terminal basic residues, is also a risk factor for this disease. Like HLA-B*27 and other AS-associated MHC-I molecules, HLA-B*40:02 binds a relatively high percentage of peptides with ERAP2-susceptible residues. In this study, the effects of ERAP2 depletion on the HLA-B*40:02 peptidome were analyzed. ERAP2 protein expression was knocked out by CRISPR in the transfectant cell line C1R-B*40:02, and the differences between the peptidomes from the wild-type and ERAP2-KO cells were determined by label-free quantitative comparisons. The qualitative changes dependent on ERAP2 affected about 5% of the peptidome, but quantitative changes in peptide amounts were much more substantial, reflecting a significant influence of this enzyme on the generation/destruction balance of HLA-B*40:02 ligands. As in HLA-B*27, a major effect was on the frequencies of N-terminal residues. In this position, basic and small residues were increased, and aliphatic/aromatic ones decreased in the ERAP2 knockout. Other peptide positions were also affected. Because most of the non-B*27 MHC-I molecules associated with AS risk bind a relatively high percentage of peptides with N-terminal basic residues, we hypothesize that the non-epistatic association of ERAP2 with AS might be related to the processing of peptides with these residues, thus affecting the peptidomes of AS-associated MHC-I molecules. ***Molecular & Cellular Proteomics 18: 2298–2309, 2019. DOI: 10.1074/mcp.RA119.001710.***

The endoplasmic reticulum aminopeptidases (ERAP)[1] and ERAP2 trim peptides in the endoplasmic reticulum (ER) to the correct size for binding the MHC-I molecules (1, 2) and can also destroy MHC-I ligands by overtrimming (3). While closely related in structure and function, both enzymes present a number of significant differences in residue specificity and substrate handling. For instance, ERAP2 shows a preference for peptides with basic residues, mainly Arg, at peptide position (P)1, although it can also trim a few other residues (2, 4), whereas ERAP1 prefers hydrophobic ones and can cleave virtually all residues except Pro, albeit with distinct efficiencies (5). In addition, ERAP1 efficiently cleaves peptides longer than the optimal size for MHC-I binding, is less efficient with 9-mers, and virtually inactive with 8-mers and smaller peptides, due to a mechanism known as *molecular ruler* (6). In contrast, ERAP2 is relatively inefficient with long peptides and becomes increasingly active with shorter ones (7).

ERAP1 and ERAP2 also show differences at the genetic level. Whereas ERAP1 is expressed in all individuals and exhibits a relatively large number of functional variants in human populations (8), ERAP2 has a much more limited polymorphism at the protein level (9), and most individuals seem to express a single allotype because the other one is in tight linkage disequilibrium with a frequent polymorphism that affects ERAP2 expression (10). Thus, homozygous individuals for this polymorphism, which amount to about 25% of the population, are ERAP2-negative.

ERAP1 and ERAP2 are risk factors for some diseases, including HLA-I-associated disorders. Both enzymes are associated with ankylosing spondylitis (AS), psoriasis, and birdshot chorioretinopathy for which HLA-B*27, HLA-C*06:02, and A*29:02, respectively, are the most prominent risk factors. ERAP2 is also associated with Crohn's disease (11), an inflammatory disorder of the gut that is most strongly associated with MHC-II, but with additional involvement of MHC-I genes (12). ERAP1, but apparently not ERAP2, is associated with Behçet's disease, for which HLA-B*51 is also a strong susceptibility factor (4, 13). Other HLA-B alleles, B*13:02, B*40:01, B*40:02, B*47:01, and B*51:01, were identified as risk factors for AS, although their association with this disease is much weaker compared with HLA-B*27 (14). The association of ERAP1 with AS is in epistasis with HLA-B*27 and B*40:01, but no epistasis has been reported, to the best of our

From the ‡Centro de Biología Molecular Severo Ochoa (CSIC-UAM), 28049 Madrid, Spain; §Centro Nacional de Microbiología, Instituto de Salud Carlos III, 28220 Majadahonda (Madrid), Spain; ¶Faculty of Biology, Technion - Israel Institute of Technology, Haifa 32000, Israel

Received August 1, 2019, and in revised form, September 2, 2019
Published, MCP Papers in Press, September 17, 2019, DOI 10.1074/mcp.RA119.001710

knowledge, for B*40:02 (14). ERAP2 is non-epistatically associated with these diseases. The identification of ERAP2 as a risk factor for AS both in HLA-B*27-positive and -negative individuals (15, 16) highlights the importance of defining the role of this enzyme in shaping the peptidomes of non-B*27 HLA-I molecules associated with AS.

The influence of ERAP2 on MHC-I-bound peptidomes has been examined so far in HLA-B*27:05 (17, 18), A*29:02 (19), and HLA-B*51:01 (20). The B*27:05 peptidome shows a relatively high frequency of peptides with basic P1 residues, and the overwhelming majority of HLA-B*27 ligands have R at P2. The major effect of ERAP2 expression on the HLA-B*27 peptidome was a quantitative decrease in the abundance of peptides with basic P1 residues, which resulted in decreased affinity of the peptidome, compared with absence of the enzyme. In A*29:02, where the frequency of basic P1 residues is lower than in HLA-B*27, the major effect of ERAP2 expression was a quantitative decrease of peptides with ERAP2-susceptible residues and an increase of hydrophobic ones at P1, without any significant alteration in global affinity. In HLA-B*51:01, which virtually does not bind peptides with basic P1 residues, the main effect of ERAP2 expression, when ERAP1 was also present, was not on P1 residue usage but instead on an increased abundance of 8-mers, relative to 9-mers and longer peptides. This study (20) also showed that, in the absence of ERAP1, ERAP2 is able to process HLA-B*51 ligands in the ER, revealing a degree of functional redundancy, which is only evident upon absence of ERAP1. These previous studies show that the effect of ERAP2 on MHC-I peptidomes, although significant in all cases, is strongly dependent on the peptide specificity of each particular MHC-I molecule.

Here we have examined the effects of ERAP2 depletion on the HLA-B*40:02 peptidome. The pattern of P1 residue usage among B*40:02 ligands (21) is similar to that in HLA-B*27 (13, 22), including a relatively high frequency of basic, A, S, and G residues. Yet, B*40:02 binds almost exclusively acidic residues, mainly E, at P2 so that its peptidome is very different from that of HLA-B*27, which binds mostly peptides with R at P2 (22–24). Thus, this study allow us to determine the role of ERAP2 on the peptidome of an HLA-I molecule associated with AS among HLA-B*27-negative individuals and to assess the relationship between the effects of this enzyme on two unrelated peptidomes with similar P1 residue usage.

EXPERIMENTAL PROCEDURES

Cell Lines—The human lymphoid cell line HMy2.C1R (C1R) expresses low levels of its endogenous HLA molecules (HLA-C*04:01 and HLA-B*35:03) on the cell surface (25). A stable C1R transfectant expressing HLA-B*40:02 (C1R-B*40:02) was previously described (21) and used here for immunopeptidomics studies. This was designated as the wild-type (WT). C1R cells are ERAP2-positive and express the ERAP1 variant Hap8 (26). All cell lines were grown in RPMI 1640 medium supplemented with 2 mM L-glutamine, 7% fetal bovine serum (Gibco, Thermo Fisher Scientific), penicillin, and streptomycin.

ERAP2 KO Generation by CRISPR—The Alt-R CRISPR-Cas9 system (Integrated DNA Technologies, Coralville, Iowa) was used to generate ERAP2 KO cells from the C1R:B*40:02 WT using specific guide RNAs targeting sequences flanking exons 5 and 6, including the substrate binding domain and active sites of the enzyme: ATACCATATCTCCCTTGCAG and CTTTGCTAATGATTTCACGT. These were designed with CRISPR MIT (http://crispr.mit.edu/) and ordered from Integrated DNA Technologies. The crRNA and tracrRNA were mixed in equimolar concentrations and heated at 80° for 10 min, cooled down at room temperature, and incubated with the Cas9 protein. After 10 min, about 2×10^5 C1R-B*40:02 cells were mixed with the crRNA:tracrRNA-Cas9 mix and electroporated with Neon Transfection System (Thermo Fisher Scientific, Waltham, Massachusetts) with three pulses of 1450 V and 10 ms. Individual clones were isolated by limiting dilution and genotyped by PCR using primer pairs mapping inside and outside of the deleted region. Two KO clones, designated as KO1 and KO3, and two unedited, ERAP2-positive, clones from the same transfection experiment, from now on referred as WT1 and WT2, were selected for further studies along with the polyclonal WT line.

Western Blotting and Flow Cytometry—The expression of ERAP1, ERAP2, and γ-tubulin proteins was analyzed by Western blotting as previously described (26) using the monoclonal antibodies 6H9, 3F5 (both from R&D Systems, Minneapolis, Minnesota) and GTU88 (Sigma-Aldrich, San Luis, Missouri), respectively.

Flow cytometry was performed as previously described (20), using the monoclonal antibodies W6/32 (IgG2a, specific for a monomorphic HLA-I determinant) (27) at 20 μg/ml and the secondary antibody goat anti-mouse IgG (H+L) FITC conjugate (Thermo Fisher Scientific). The fluorescence was analyzed in a FACSCanto Flow Cytometer (BD Biosciences, San Diego).

*Isolation of HLA-B*40:02-Bound Peptides and Mass Spectrometry*—HLA-B*40-bound peptides were isolated from three independent preparations of 1×10^9 cells of each cell line as previously described (28) to provide biological replicates. Briefly, cells were lysed with 150 mM NaCl, 20 mM Tris/HCl, pH 7.5, 1% Igepal CA-630 (Sigma-Aldrich), and a protease inhibitor mixture (Roche). After centrifugation, the supernatant was passed first through a precolumn with CNBr-activated Sepharose 4B (GE Healthcare) to remove unspecific interactions and then through a column containing W6/32 bound to CNBr-activated Sepharose. Next, the columns were successively washed with 20 column volumes each of 20 mM Tris/HCl, pH 8.0, containing: (1) 150 mM NaCl, (2) 400 mM NaCl, (3) 150 mM NaCl, and (4) buffer without NaCl. The MHC-bound peptides were eluted with 1% trifluoroacetic acid (Sigma-Aldrich), filtered through a Vivaspin 2 filter (cutoff 5000 Daltons) (Sartorius Stedim Biotech) and concentrated in a SpeedVac (Savant; DJB Labcare). Samples were analyzed in a Q-Exactive-Plus mass spectrometer (Thermo Fisher Scientific) as previously described (28). The peptides were resolved with a 7–40% acetonitrile gradient with 0.1% formic acid for 180 min and 0.15 μl/min on a capillary column pressure-packed with Reprosil C18-Aqua (Dr. Maisch, GmbH, Ammerbuch-Entringen, Germany) as in (29). The dynamic exclusion was set to 20 s. The selected masses were fragmented from the survey scan of the mass-to-charge ratio (m/z) 300-1800 AMU at a resolution of 70,000. MS/MS spectra were acquired beginning at m/z 200 with a resolution of 17,500. The target value was set to 1×10^5, and the isolation window to 1.8 m/z. Peptide sequences were assigned from the MS/MS spectra as described below.

[1] The abbreviations used are: ERAP, endoplasmic reticulum aminopeptidase; MHC-I, major histocompatibility complex class I; AS, ankylosing spondylitis; ER, endoplasmic reticulum; WT, wild-type; KO, knockout; IR, intensity ratio.

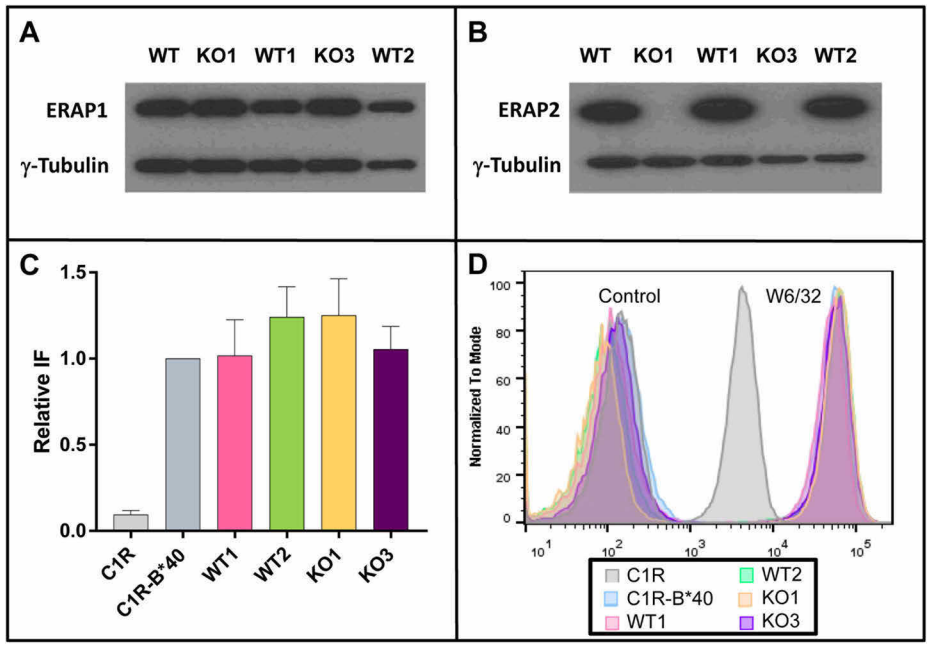

FIG. 1. **ERAP, ERAP2, and surface HLA-B*40:02 expression.** Western blotting of (*A*) ERAP1 and (*B*) ERAP2 expression in the indicated cell lines. Gamma-tubulin was used as a loading control. (*C*) HLA class I expression relative to the WT in the indicated cell lines assessed by flow cytometry. Data are mean values ± s.d. from four independent experiments. No statistically significant differences, assessed with the Student's *t* test, were found. (*D*) Representative histograms of the surface HLA class I expression, assessed with the W6/32 monoclonal antibody.

Affinity and Hydropathy Analyses—The theoretical binding affinity of HLA-B*40:02 ligands was estimated using the NetMHCcons 1.1 Server (http://www.cbs.dtu.dk/services/NetMHCcons/) as described (30). The hydropathy index of Kyte and Doolittle (31) was used for amino acid residues.

Statistical Analyses—Differences in residue frequencies were analyzed using the χ^2 test with Bonferroni correction when applicable. Relative intensity differences among peptide sets were assessed by an unpaired *t* test. Differences in the theoretical affinity of peptides were assessed by the Mann-Whitney test. In all cases $p < 0.05$ was considered as statistically significant.

Experimental Design and Strategy—The effects of ERAP2 depletion on the HLA-B*40:02 peptidome were analyzed by quantitative label-free MS. Three independent preparations of the HLA-B*40:02-bound peptides were obtained from each of the cell lines in this study and used as biological replicates, whose reproducibility was assessed by Pearson correlation analyses (Fig. S1). The peptide pools from each individual preparation were separately subjected to MS, and individual peptides were identified from the MS/MS spectra using the MaxQuant software (version 1.5.8.3) (32) with the Andromeda search engine (33) and the human UniProt/Swiss-Prot database (release 27-07-18: 732,101 entries) under the following parameters: precursor ion mass and fragment mass tolerance 20 ppm, false discovery rate 0.01 and peptide-spectrum matching false discovery rate 0.05, oxidation (Met), acetylation (protein N terminus) and Gln to Pyro-Glu conversion were included as variable modifications. No fixed modifications were included. Identifications derived from the reverse database and known contaminants were eliminated. In addition, the following peptides were selected out: (1) peptides outside the length range of 8 to 13 amino acid residues, where the large majority of MHC-I ligands are included, (2) peptides identified from untransfected C1R cells both in a previous study (34) and in a control experiment in which peptides from untransfected C1R cells were identified using the same conditions described in the present study, (3) peptides with canonical anchor residues at P2 corresponding to the endogenous MHC-I molecules of C1R, that is peptides with Pro2 (B*35:03), Phe2 or Tyr2 (C*04:01), and (4) peptides with very low theoretical affinity (IC50 > 10,000 nM), which showed up as a clearly distinct subset from the bulk of the canonical B*40:02 ligands (Fig. S2).

Because a majority of the identified peptides were found in both the WT and KO cells (Fig. S3), quantitative differences in peptide amounts between cell lines were assigned in pairwise comparisons as follows (20): In each experiment the intensity of any given ion peak was normalized to the total intensity of all the identified B*40:02 ligands. The mean normalized intensity of each ion peak from the three individual experiments for each cell line was taken as the amount of that peptide relative to the total amount of ligands identified in that cell line. The HLA-B*40:02 ligands in each pairwise comparison were classified based on the normalized intensity ratio (IR) of the corresponding ion peak in the two cell lines. Peptides predominant in one cell line, relative to the other (IR>1.0) were subdivided in two subsets. Peptides with IR>1.0 to 1.5 (hereafter abbreviated as IR>1.0–1.5) in either cell line were considered to be expressed in similar amounts in the two cell lines, and therefore little or no affected by ERAP2. Peptides with IR>1.5 in one cell line relative to the other, including peptides found only in that cell line, were considered to be up-regulated in that cell line and consequently influenced by the ERAP2 context. The relationship of this classification to the statistical significance of the differences in peptide amounts was established by means of volcano plots for each pairwise comparison (Fig. S4).

RESULTS

*ERAP1, ERAP2, and HLA-B*40:02 Expression on WT and ERAP2 KO Lines*—The polyclonal C1R-B*40:02 transfectant cell line, WT, two unedited clonal lines obtained by limiting dilution from the CRISPR-subjected WT line, WT1 and WT2, and two clonal ERAP2 KO lines, KO1 and KO3, were used. The latter lacked any detectable expression of the ERAP2 protein, but their expression of ERAP1 remained unaltered (Figs. 1*A* and 1*B*). The surface levels of B*40:02, as assessed by flow cytometry with the W6/32 monoclonal antibodies, were similar in both the WT and KO cells (Figs. 1*C* and 1*D*).

*The HLA-B*40:02 Peptidome in ERAP2-Proficient and Deficient Cells*—A total of 9,593 peptides were assigned as B*40:02 ligands from the three WT and two KO lines used in

this study, of which 7887, 8042, 8608, 8091, and 8126 were identified in the WT, WT1, WT2, KO1, and KO3, respectively (Table S1). A large majority of the peptides was found both in the presence and in the absence of ERAP2 (Fig. S3). Yet, of 7222 peptides found in all three WT, WT1, and WT2 lines, 427 (5.9%) were not found in any of the KO1 and KO3 lines. Conversely, of 7547 peptides found in both KO1 and KO3 cells, 375 (5.0%) were not found in any of the three WT lines. Thus, ERAP2 expression may qualitatively determine the differential presentation of at least 5–6% of the B*40:02 peptidome, a figure that is similar to the reported effects of ERAP2 expression on HLA-B*27 ligands (17).

The length distribution of all the B*40:02 ligands was: 9.3% of 8-mers, 61.6% of 9-mers, 15.9% of 10-mers, and 9.2% >10-mers, with very small differences among cell lines, regardless of the presence or absence of ERAP2. Yet, when the global intensity of the ion peaks corresponding to the peptides of a given length in each cell line was considered, a moderate increase of the total amount of octamers could be detected in ERAP2 KO cells (12.9–15.6%) relative to ERAP2-proficient cells (9.6–10.4%), with p values ranging from 0.018 to 2.7E-04. Intensity differences among 9-mers and larger peptides were not consistent between WT and KO cell lines (Fig. S5).

*Quantitative Effects of ERAP2 Depletion on the B*40:02 Peptidome*—These were addressed in pairwise comparisons involving the WT/KO1 and WT/KO3 cell line pairs. The peptides from each cell line with IR>1.5 relative to the other were compared, focusing on several peptide features that will be detailed below. Parallel comparisons were also carried out between the corresponding IR>1.0–1.5 subsets, as an internal control. When appropriate, the specificity of these changes was further assessed by analogous comparisons involving the WT1 and/or WT2 clonal lines. The number of peptides in each subset for every comparison between cell line pairs is given in Table I.

An estimation of the overall quantitative effects of ERAP2 on the peptidome was obtained from the percentage of shared peptides up-regulated in each cell line in the various pairwise comparisons: those with $p < 0.05$ in the volcano analyses (Fig. S4). As shown in Table II, the control comparisons (WT/WT1, WT/WT2, WT1/WT2, and KO1/KO3) showed an average of 15.3% altered peptides (range 10.5–18.5%), which can be considered as ERAP2-independent cell-to-cell changes. In contrast, the comparisons between cell lines differing in ERAP2 expression (WT/KO1, WT/KO3, WT1/KO1, WT1/KO3, WT2/KO1, and WT2/KO3) showed an average of 50.0% altered peptides (range 41.9–57.1%). Thus, ERAP2-dependent quantitative alterations in the B*40:02 peptidome can be estimated to affect about 35% of the peptidome.

The quantitative effects in the B*40:02 peptidomes were assessed mainly on the basis of the following features: (1) changes in P1 residue frequencies, (2) changes at peptide positions downstream the N terminus, (3) differences in the frequencies of N-terminal flanking (P-1) residues, (4) hydrophobicity differences, and (5) theoretical affinity differences.

Effects of ERAP2 Depletion on Peptide Length—A comparison of the IR>1.5 subsets from WT and KO1 or KO3 showed

TABLE I
*Classification of B*40:02 ligands in pairwise comparisons*

	Total	Shared	Specific[a]	IR>1.5[b]	IR>1.0–1.5
WT	7887	7380	507	2272	2335
WT1	8042	7380	662	1855	2087
WT	7887	7565	322	1812	2340
WT2	8608	7565	1043	2528	2250
WT	7887	6911	976	3630	1140
KO1	8091	6911	1180	3259	1038
WT	7887	6922	965	3700	1159
KO3	8126	6922	1204	3165	1067
WT1	8042	7036	1006	3587	1182
KO1	8091	7036	1055	3311	1017
WT1	8042	7038	1004	3734	1192
KO3	8126	7038	1088	3225	979
WT2	8608	7408	1200	4067	1203
KO1	8091	7408	683	2922	1099
WT2	8608	7439	1169	4118	1310
KO3	8126	7439	687	2799	1068
WT1	8042	7785	257	807	2503
WT2	8608	7785	823	1707	3848
KO1	8091	7547	544	1619	3068
KO3	8126	7547	579	1347	2636

[a]Peptides found only in one of the two cell lines compared.
[b]This subset includes the shared peptides with IR>1.5 relative to the other cell line plus those found only in the corresponding cell line of the two being compared ("specific").

TABLE II
*Quantitative differences in the expression of B*40:02 ligands between cell lines*

Comparison	No. of shared peptides[a]	$p < 0.05$[b]	% altered[c]
WT vs WT1	5890	941	**16.0**
WT vs WT2	5978	981	**16.4**
WT1 vs WT2	6652	701	**10.5**
KO1 vs KO3	6400	1183	**18.5**
WT vs KO1	5388	2440	**45.3**
WT vs KO3	5292	2216	**41.9**
WT1 vs KO1	5840	3203	**54.8**
WT1 vs KO3	5746	2842	**49.5**
WT2 vs KO1	6249	3566	**57.1**
WT2 vs KO3	6123	3153	**51.5**

[a]Total number of shared peptides included in the volcano analyses shown in Fig. S4.
[b]Numbers of peptides showing statistically significant differences in their expression level between the cell lines compared.
[c]Percentage of peptides showing statistically significant differences in their expression level between the cell lines compared.

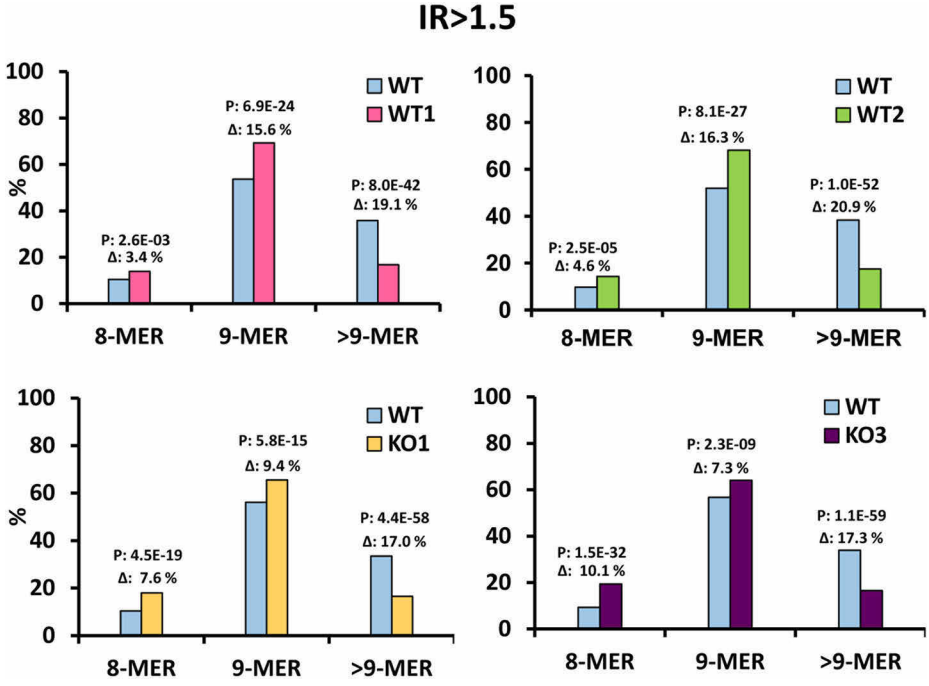

FIG. 2. **Quantitative effects of ERAP2 depletion on the length of B*40:02 ligands.** Comparison of the peptides with IR>1.5 from the indicated cell lines. In this and all other figures these subsets include both shared peptides overrepresented plus those found only in the corresponding cell line of the two being compared. The changes in the percentage frequency of peptides according to their length between the polyclonal and monoclonal WT lines (*upper panels*) and between WT and the ERAP2 KO lines (*lower panels*) are shown. Statistically significant differences were calculated using the χ^2 test with Bonferroni correction, and their *p* values are indicated. Percent differences between peptides on the same length in each comparison (Δ) are also indicated in all cases. The numbers of peptides compared (Table I) are the following: WT/WT1, 2272/1855; WT/WT2, 1812/2528; WT/KO1, 3630/3259; WT/KO3, 3700/3165.

an increased frequency of 8-mers and 9-mers, at the expense of longer peptides, in the absence of ERAP2. A similar pattern was observed in the WT/WT1 and WT/WT2 comparisons (Fig. 2) indicating that these differences were mostly unrelated to ERAP2. Yet, the increased frequency of octamers in KO1 relative to WT (+7.6%, p: 4.5E-19) and KO3 relative to WT (+10.1%, p: 1.5E-32) was larger than the corresponding increase in WT1 or WT2, relative to WT (+3.4%, p: 2.6E-03 and +4.6%, p: 2.5E-05, respectively). This suggests that depletion of ERAP2 results in a moderate increase of 8-mers. This occurs at the expense of 9-mers, as reflected in the smaller differences in 9-mer frequencies in WT/KO1 and WT/KO3, relative to the WT/WT1 and WT/WT2 comparisons, and in the corresponding 9-mer/8-mer ratios, which were 5.4 and 6.1 in the WT and 3.6 and 3.3 in KO1 and KO3, respectively, whereas no differences in these ratios were observed in the WT/WT1 and WT/WT2 comparisons (Fig. 2). No statistical differences were found among the peptides in the IR>1.0–1.5 subsets (Fig. S6).

Length-Dependent Effects of ERAP2 Depletion on N-Terminal Residue Usage—A comparison of the IR>1.5 subsets from WT and KO1 or KO3 showed drastic alterations in P1 residue frequencies between both subsets (Fig. 3*A*). In the absence of ERAP2, the following residues were increased in KO1, relative to WT: R (3.4-fold), K (4-fold), A (2.1-fold), S (1.5-fold), and G (2-fold). These results were closely reproduced in the WT/KO3 comparison as well as in analogous comparisons involving the clones WT1 and WT2 instead the polyclonal WT line (Fig. S7) and were very attenuated or absent when the IR>1.0–1-5 subsets were compared (Fig. 3*B*).

P1 alterations were variable as a function of peptide length: in the absence of ERAP2, K was increased among peptides of all lengths from the IR>1.5 subsets, R was increased among 9-mers and 10-mers, but not in 8-mers, the differential frequencies of S and G were maximal among 8-mers, and A, S, and G were not increased, or were even less frequent, among 10-mers (Fig. 4). These differences were attenuated or absent among the IR>1.0–1.5 subsets (Fig. S8).

Taken together these results indicate a selective action of ERAP2 on decreasing the amounts of peptides with basic (R, K) and small residues (A, S, G) following distinct length-dependent patterns.

*ERAP2 Depletion Affects P3 Residue Usage among B*40:02 Ligands*—Another peptide position showing a consistent effect of ERAP2 was P3. Both in the WT/KO1 and WT/KO3 comparisons, peptides in the IR>1.5 subsets from the WT showed statistically significant increase of K, G, D, and E at P3, whereas aliphatic residues were increased in the corresponding subsets from KO1 and KO3 (Fig. 5). The same differences were consistently observed when WT clones, instead the polyclonal WT line, were compared with both KO clones (Fig. S9). Some additional differences observed in these latter comparisons did not show a consistent pattern, suggesting that they were cell line-, rather than ERAP2-dependent (e.g., H only in comparisons involving KO1, R only in those involving WT1, etc.). Most of these changes did not reach statistical significance among the IR>1.0–1.5 subsets. The changes in P3 frequencies showed the same tendency on 8-mers, 9-mers, and 10-mers from the IR>1.5 subsets, although among 10-mers did not generally reached statistical

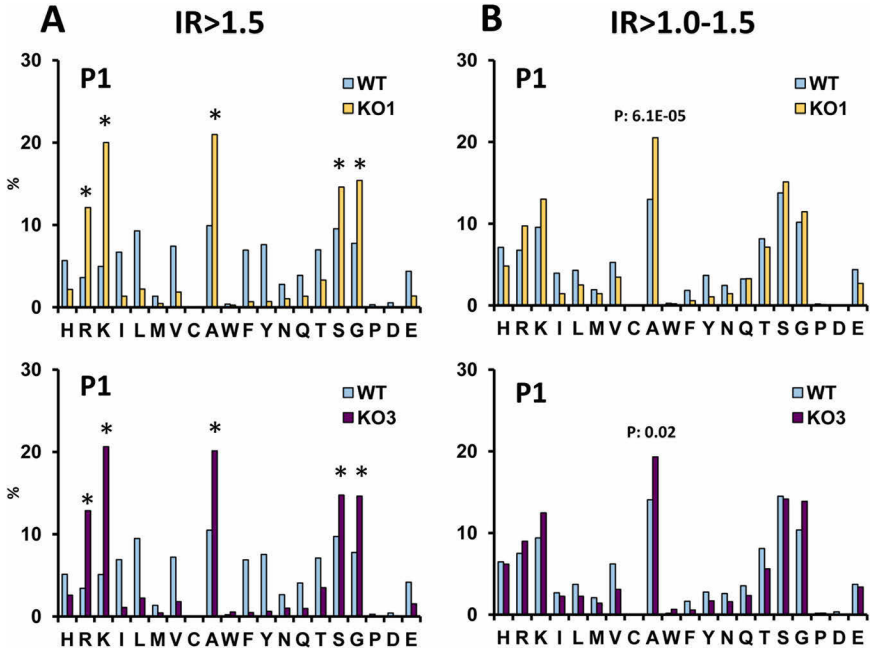

FIG. 3. **Quantitative effects of ERAP2 depletion on N-terminal residue frequencies among HLA-B*40:02 ligands.** (*A*) Comparison of the P1 residue frequencies among peptides with IR>1.5 from the indicated cell lines. The numbers of peptides compared (Table I) are the following: WT/KO1, 3630/3259; WT/KO3, 3700/3165. Statistically significant differences were calculated using the χ^2 test with Bonferroni correction. Residues statistically increased in the absence of ERAP2 are labeled with (*). The corresponding *p* values in the WT/KO1 and WT/KO3 are the following: R, 1.1E-38 and 2.7E-46; K, 5.2E-80 and 1.9E-83; A, p: 5.5E-36 and 1.6E-27; S, 2.2E-09 and 4.6E-09; G, 6.5E-22 and 3.8E-18. (*B*) Comparison of the P1 residue frequencies among peptides with IR>1.0–1.5 from the same cell lines. The numbers of peptides compared (Table I) are: WT/KO1, 1140/1038; WT/KO3, 1159/1067. Residues statistically increased in the absence of ERAP2 are indicated by their corresponding *p* values. Other differences were not significant or were increased in the presence of ERAP2.

significance (Fig. S10). No differences were found among the corresponding IR>1.0–1.5 subsets (Fig. S11).

Effects of ERAP2 Depletion on Other Peptide Positions—This was analyzed on 9-mers because these are the most numerous B*40:02 ligands of homogeneous length, which is required for proper alignment of most internal positions. When the IR>1.5 subsets from WT and KO1 or KO3 were examined statistically significant differences between residues at positions other than P1 and P3 were observed at all other positions (Table S2), but they were generally occasional. An exception was P5 where hydrophobic residues (I, L, F) were increased in the WT (by about 1.8–1.9-fold) whereas polar ones (S, T) and Pro were increased in KO cells (Fig. 6). Thus, although ERAP2 expression directly concerns trimming of only P1 residues, the enzyme also affects residue usage at other peptide positions.

*ERAP2 Depletion Alters the Hydrophobicity of B*40:02 Ligands at Multiple Positions, But Not Their Global Affinity*—The hydropathy of B*40:02 ligands at individual positions was compared between the peptides in the IR>1.5 subsets from WT *versus* KO1 and WT *versus* KO3 cells. These comparisons were done with all the peptides for P1 and P3 (Fig. S12*A*) because these positions can be properly aligned regardless of peptide length, and with 9-mers only when all peptide positions were compared (Fig. S12*B*). As expected from the nature of the altered residues, hydrophobicity was decreased at P1 and increased at P3 upon ERAP2 depletion. In addition, a lower hydrophobicity was observed at P5 and other positions among 9-mers. These changes did not influence the global affinity of the B*40:02 peptidome, as demonstrated by the similar values in the IR>1.5 subsets from the WT and KO1 or KO3 lines (Fig. S12*C*).

Effects of ERAP2 Depletion on N-Terminal Flanking Residues—A way of assessing the influence of ERAP2 on the generation of B*40:02 ligands is by comparing the frequencies of the P(-1) residues in their parental proteins. Thus, the frequency of these residues among the IR>1.5 subsets from the WT/KO1 and WT/KO3 cell line pairs was compared for peptides of the same length in both subsets. The only consistent differences in both comparisons were observed among 8-mers, where R and G were decreased, and F was increased, in the absence of ERAP2 (Fig. 7**)**. This result suggests that ERAP2 favors the generation of 8-mers from N-extended precursors with at least R and G. The relatively small numbers of 8-mers in these subsets limits the statistical power of the comparison, so that additional effects on other P(-1) residues are not ruled out. No statistical differences were observed between 9-mers or 10-mers in these subsets, except L among 9-mers in WT/KO1 (p: 0.02) but not in WT/KO3. Lack of differential P(-1) usage on peptides longer than 8-mers is consistent with the lower cleavage efficiency of

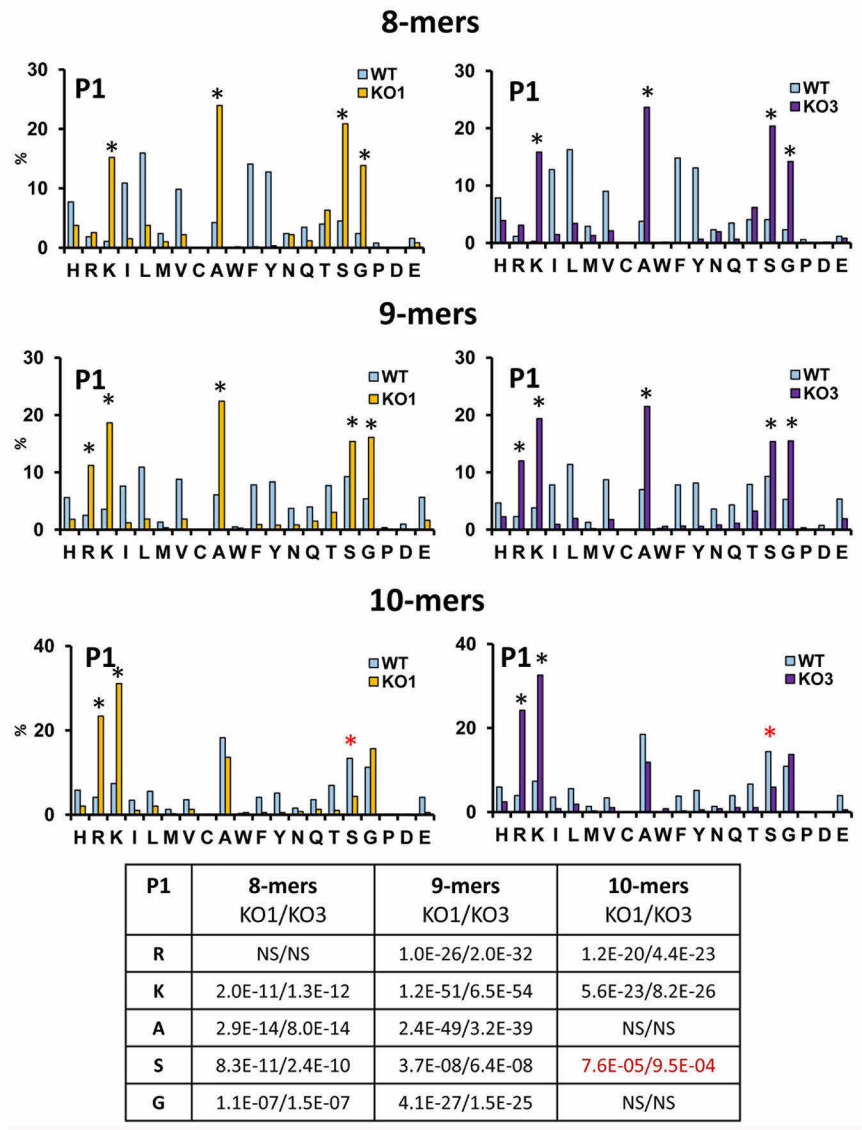

P1	8-mers KO1/KO3	9-mers KO1/KO3	10-mers KO1/KO3
R	NS/NS	1.0E-26/2.0E-32	1.2E-20/4.4E-23
K	2.0E-11/1.3E-12	1.2E-51/6.5E-54	5.6E-23/8.2E-26
A	2.9E-14/8.0E-14	2.4E-49/3.2E-39	NS/NS
S	8.3E-11/2.4E-10	3.7E-08/6.4E-08	7.6E-05/9.5E-04
G	1.1E-07/1.5E-07	4.1E-27/1.5E-25	NS/NS

FIG. 4. **Quantitative effects of ERAP2 depletion on N-terminal residue frequencies among HLA-B*40:02 ligands as a function of peptide length.** Comparison of the P1 residue frequencies among 8-mers (*upper panels*), 9-mers (*intermediate panels*) and 10-mers (*lower panels*) with IR>1.5 from the indicated cell lines. The numbers of peptides compared were as follows. WT/KO1: 376/585 (8-mers), 2038/2136 (9-mers), and 701/389 (10-mers); WT/KO3: 344/613 (8-mers), 2100/2028 (9-mers), and 735/371 (10-mers). Statistically significant differences were calculated using the χ^2 test with Bonferroni correction. Residues statistically increased in the absence of ERAP2 in each comparison are labeled with (*), and their *p* values are shown in the table at the bottom. The statistically significant decrease of S among 10-mers, and the corresponding *p* values in the WT/KO1 and WT/KO3 comparisons are labeled in red. Other differences were not significant or were increased in the presence of ERAP2.

ERAP2 with substrates of increased length. The IR>1.0–1.5 subsets showed no statistical differences in P (-1) residues.

DISCUSSION

A remarkable feature of the association of ERAP2 with AS is that, unlike ERAP1, there is no epistasis with HLA-B*27 because ERAP2 is associated with AS among HLA-B*27 positive and negative individuals (16). HLA-B*40:02 is one of a small group of non-B*27 HLA-B allotypes conferring risk to AS (14) independently of HLA-B*27. Like the latter, HLA-B*40:02 has a high percentage of basic P1 residues, which are known targets of ERAP2. However, due to the strong preference for acidic P2 residues the B*40:02 peptidome is quite distinct from that of HLA-B*27, which mainly binds peptides with R at this position (22–24).

The effects of ERAP2 on MHC-I bound peptidomes is insufficiently characterized, although the role of this enzyme on HLA-B*27:05 (17, 18), HLA-A*29:02 (19), and HLA-B*51:01 (20) has been reported. These studies showed that the major effects of ERAP2 are quantitative, influencing peptide amounts, and allotype dependent. For instance, in B*27:05 the presence of ERAP2 lead to a moderate increase on the amounts of 9-mers at the expense of longer peptides, a decrease of peptides with basic P1 residues, and a globally decreased affinity of the peptidome (17, 18). In contrast the influence of ERAP2 on the A*29:02 peptidome resulted in lower amounts of 9-mers and higher amounts of longer peptides, an increase of hydrophobic, ERAP2-resistant, P1 residues, and moderately increased global affinity of the peptidome (19). The influence of ERAP2 on the peptidome of HLA-B*51:01, a molecule that binds an unusually high percentage of 8-mers and lacks ligands with P1 basic residues (28), was dependent on ERAP1. In the presence of this enzyme, ERAP2 expression resulted in a remarkable

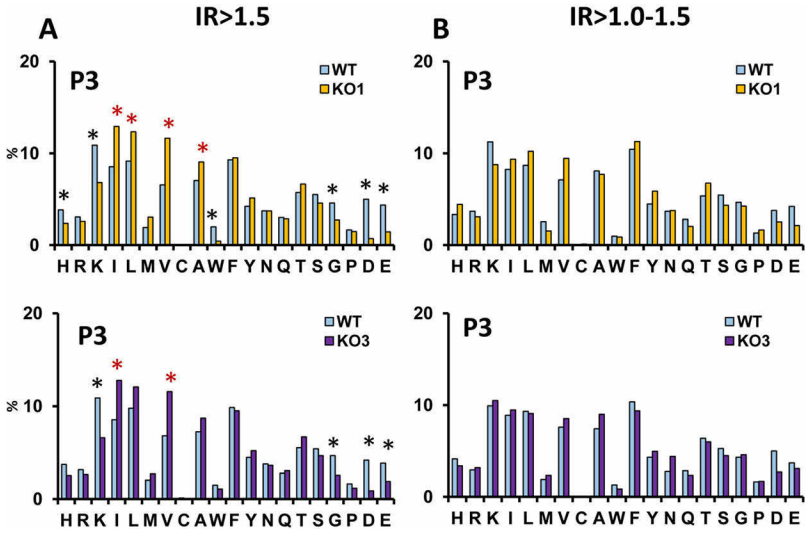

FIG. 5. **Quantitative effects of ERAP2 depletion on residue frequencies at P3 among HLA-B*40:02 ligands.** (*A*) Comparison of the P3 residue frequencies among peptides with IR>1.5 from the indicated cell lines. The numbers of peptides compared (Table I) are the following: WT/KO1, 3630/3259; WT/KO3, 3700/3165. Statistically significant differences were calculated using the χ^2 test with Bonferroni correction. Residues statistically increased in the absence or in the presence of ERAP2 are labeled red or black asterisks, respectively. The *p* values corresponding to the residues showing statistical differences in both comparisons were the following: K (9.1E-08, 1.3E-08), I (9.7E-08, 3.1E-07), V (5.0E-12, 1.9E-10), G (1.4E-03, 9.9E05), D (5,3E-24, 9.1E-16), E (4.2E-11,4.5E-05). (*B*) Comparison of the P3 residue frequencies among peptides with IR>1.0–1.5 from the same cell lines. The numbers of peptides compared (Table I) are: WT/KO1, 1140/1038; WT/KO3, 1159/1067. No statistical differences were observed.

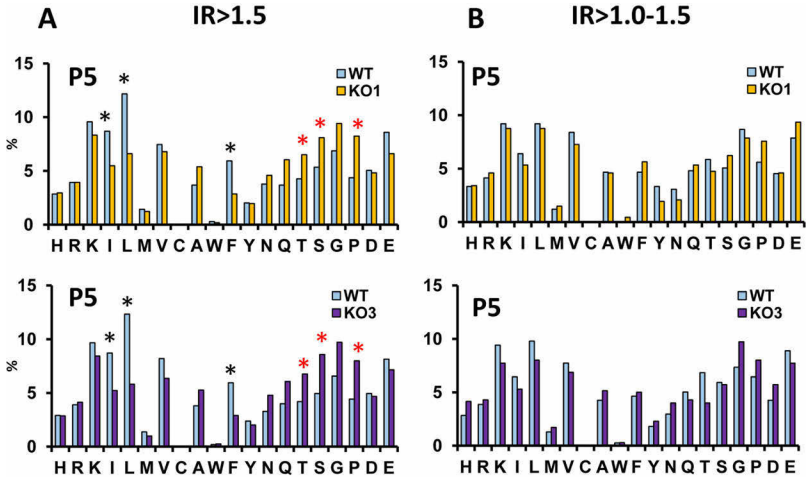

FIG. 6. **Quantitative effects of ERAP2 depletion on residue frequencies at P5 among HLA-B*40:02 nonamer ligands.** (*A*) Comparison of the P5 residue frequencies among 9-mers with IR>1.5 from the indicated cell lines. The numbers of peptides compared are the following: WT/KO1, 2038/2136; WT/KO3, 2100/2028. Statistically significant differences were calculated using the χ^2 test with Bonferroni correction. Residues statistically increased in the absence or in the presence of ERAP2 are labeled red or black asterisks, respectively, and their *p* values are shown in Table S2. (*B*) Comparison of the P5 residue frequencies among peptides with IR>1.0–1.5 from the same cell lines. The numbers of peptides compared were: WT/KO1, 750/674; WT/KO3, 776/699. No statistical differences were observed.

increase in the amounts of 8-mers, at the expense of 9-mers and longer peptides, with little effect on P1 residue usage and affinity. These effects on peptide length, which are opposite to those observed among B*40:02 ligands, were interpreted as resulting from the absence of basic P1 residues and the high frequency of Pro at P2 among B*51:01 ligands (20). An effect of ERAP2 on favoring the generation of B*51:01 ligands with basic N-terminal flanking residues was also detected (20). Together these studies revealed an influence of ERAP2 that was distinct from that of ERAP1, but dependent on the presence of this enzyme and concordant with the substrate specificity described *in vitro* (2, 4). Yet, the binding preferences of each MHC-I allotype determine, at the end, the effects of ERAP2 on both peptide generation and destruction for each particular peptidome.

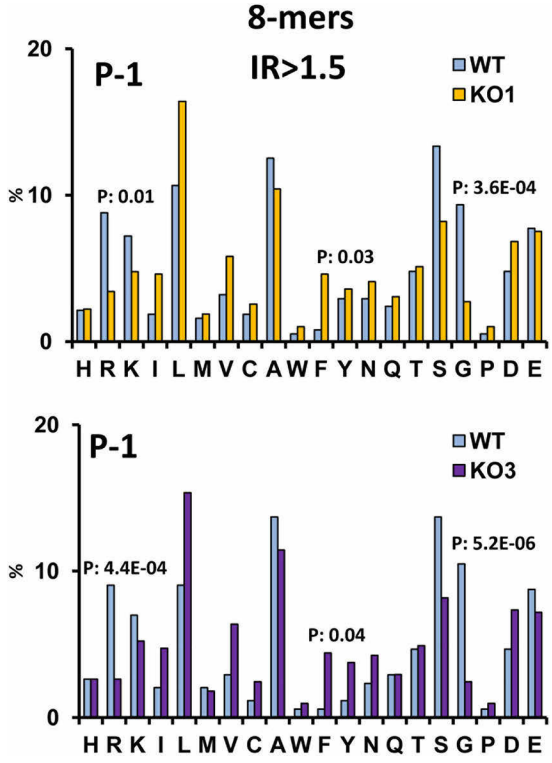

FIG. 7. **ERAP2-dependent differential frequencies of N-terminal flanking residues among B*40:02 octamers.** Comparison of the P(-1) residue frequencies among 8-mers in the IR>1.5 subsets from WT/KO1 (upper panel: N. of peptides, 376 and 585, respectively) and WT/KO3 (lower panel: N. of peptides: 344 and 613, respectively). Statistically significant differences were calculated using the χ^2 test with Bonferroni correction and their *p* values are indicated.

A comparison of the effects of ERAP2 on the B*40:02 and B*27:05 peptidomes is warranted due to the association of both molecules with AS, albeit with largely different strength. Both similarities and differences are observed. For instance, in B*40:02 the presence of ERAP2 resulted in lower 8-mer amounts, and a concomitant increase of 9-mers, relative to absence of this enzyme, as reflected in the corresponding 9-mer/8-mer ratios. This was not observed on B*27:05, which binds very few 8-mers (17, 18). A major similarity between the effects of ERAP2 expression on the B*27:05 and B*40:02 peptidomes is on the diminishment of basic P1 residues, which are highly susceptible to ERAP2 trimming and relatively frequent in both allotypes. In B*40:02 the joint frequency of R and K at P1 among peptides up-regulated in the presence of ERAP2 (IR>1.5 subset) was about 8.5% whereas in the absence of this enzyme was about 33% (3.9-fold increase). In B*27:05, the corresponding figures were 19.6 to 27.5% in the presence of ERAP2 and about 45% in the absence of this enzyme (about 1–6 to 2.3-fold increase) depending on the cell lines compared (17). Thus the effect of ERAP2 on peptides with basic P1 residues was even higher in B*40:02 than in B*27:05. However, a notorious difference between both molecules was observed in the effects of ERAP2 on the frequencies of G, A, and S at P1. Whereas in B*27:05 the frequencies of these residues were not consistently affected by ERAP2 and, if at all, they were higher in the presence of the enzyme (17, 18), these three residues were significantly decreased among B*40:02 ligands in the presence of ERAP2, particularly among 8-mers and 9-mers. Overall, the effects of ERAP2 on P1 residue usage were larger than in HLA-B*27 and introduced extensive quantitative changes in the B*40:02 peptidome affecting a larger diversity of peptides.

The decreased frequency of R, K, A, G, and S at P1 among B*40:02 ligands in the presence of ERAP2 was associated with a concomitant increase of other P1 residues, including aliphatic an aromatic ones, which are generally susceptible to ERAP1 trimming. This was not observed in B*27:05 (17, 18). Whereas these differences might be somehow influenced by distinct P1 residue preferences for binding to B*27:05 or B*40:02 other explanations, not mutually exclusive, may be considered. Whereas A may be cleaved by ERAP2, G and S are not or very poorly cleaved by this enzyme *in vitro* (4). However, 10-mer substrates were used in that study. It is conceivable that residues such as A, G, and S, may be more efficiently cleaved on shorter substrates, as suggested by the alterations in the frequencies of these residues, which were observed on 9-mers and, more so, on 8-mers, but not among longer peptides. Another possibility is that the higher frequencies of A, G, and S at P1 among B*40:02 ligands in the absence of ERAP2 could be, to some extent, a consequence of increased trimming of hydrophobic residues by ERAP1 when ERAP2 is not present. The putative inhibitory effect of ERAP2 on ERAP1 trimming could be because the 8-mers resulting from cleavage of nonameric B*40:02 ligands cannot be further degraded by ERAP2 due to their acidic motif at P2. Because 8-mers can inhibit ERAP1 trimming of longer substrates (35), this could result in increased cleavage of the ERAP1-susceptible hydrophobic P1 residues in the absence of ERAP2. This inhibition would not take place among HLA-B*27 ligands, at least to the same extent, because the ERAP2-susceptible R motif at P2 of these peptides imply that the octamers resulting from degradation of nonameric B*27:05 ligands would be further degraded by ERAP2. This would explain why A, G, and S at P1 were not altered among HLA-B*27 ligands as a function of ERAP2. An inhibitory effect of 8-mers on ERAP1 trimming would also be compatible with the observed increase of 8-mer amounts upon ERAP2 depletion, as a consequence of favored ERAP1-mediated overtrimming of nonameric B*40:02 ligands. However, the lower amounts of 8-mers in the presence of ERAP2 can also be explained by the efficient ERAP2-mediated trimming of these short peptides

Indeed, ERAP1 inhibition mediated by ERAP2 hardly explains that the highest increase of A, G, and S at P1 upon ERAP2 depletion were observed on 8-mers, which are rarely cleaved by the former enzyme. As discussed above, the effects on 8-mers are better explained by direct trimming of

these residues by ERAP2. It is possible that both mechanisms will operate to different extent on 8-mers and 9-mers, the inhibitory effect being particularly relevant on the latter peptides. For substrates longer than 9-mers, ERAP2 would become very inefficient in cleaving A, G, and S residues and the proposed 8-mer-mediated inhibition of ERAP1 would obviously not take place on these longer substrates.

Whereas the proposed mechanism of ERAP1 inhibition of 9-mer over-trimming by their 8-mer products explains the distinct patterns of ERAP2-dependent P1 residue changes among HLA-B*27 and B*40:02 ligands and is compatible with observations *in vitro* (35), it remains highly hypothetical and needs to be substantiated by further research.

The ERAP2-dependent changes at positions downstream the N terminus among B*40:02 ligands might have arisen to compensate for the changes in affinity, due to the alterations at P1. This would explain that the B*40:02 peptidomes expressed in the presence or absence of ERAP2 showed no significant changes in affinity, a situation different from that on B*27:05 (18).

In addition to the alterations due to epitope destruction, ERAP2 had an effect on epitope generation that was revealed only on 8-mers with the N-terminal flanking residues of R and G. The fact that the effect was apparent only on 8-mers is fully consistent with the higher activity of this enzyme on short peptides.

In summary the effects of ERAP2 on the B*40:02 peptidome are considerably different from those on HLA-B*27 but are analogous in the effect on peptides with N-terminal basic residues, which are frequent in both peptidomes. A role of HLA-B*27 ligands with basic P1 residues in AS was previously hypothesized based on the particular resistance of peptides with dibasic N-terminal sequences to many aminopeptidases (36). Thus, the association of ERAP2 with AS might be related to alterations by this enzyme on the presentation of peptides with basic P1 residues by MHC-I allotypes that present a substantial percentage of such peptides. In support of this idea it is noteworthy that, with the exception of B*51:01, all other non-B27 HLA-B allotypes that confer risk to AS: B*40:01, B*40:02, B*13:02, and B*47:01 (14) have, like HLA-B*27, acidic (E) residues at the A pocket positions 63 and 163 (International Immunogenetics Project/HLA database: https://www.ebi.ac.uk/ipd/imgt/hla, and bind a significant percentage of peptides with basic P1 residues (Immunoepitope database: https://www.iedb.org). This might help to explain the non-epistatic nature of the association of ERAP2 with AS if a mechanism based on destruction of MHC-I ligands with N-terminal basic residues, without excluding the generation of ERAP2-dependent epitopes, were assumed for the pathogenetic role of this enzyme in AS.

Three features of HLA-B*27 have been proposed to explain its association with AS: the involvement of specific peptide epitopes (37), the capacity of HLA-B*27 to misfold and trigger an unfolded protein response (38), and the presentation of HLA-B*27 heavy chain homodimers at the cell surface (39), that can be recognized by NK cells and by a subset of Th17 cells (40). Whereas all these features might possibly be affected by the alterations induced in HLA-B*27 by both ERAP1 and ERAP2 (13), neither misfolding nor the formation of heavy chain homodimers would seem to explain the association of B*40:02 with AS or the influence of ERAP2 on the B*27-negative disease. B*40:02 is not known to misfold in the ER or to trigger unfolded protein responses, and ERAP2 expression did not significantly alter the global affinity of its peptidome in our study. Moreover, B*40:02 lacks the Cys67 residue, which is involved in the formation of cell surface homodimers (39). Thus, the AS-predisposing effect of ERAP2 seems, on the basis of our observations, more compatible with either the destruction of putative protective epitope(s) or the generation of pathogenic one(s). Whereas we consider this effect as the most likely one for the involvement of ERAP2 in the B*27-negative AS, we do not rule out that the effects of this enzyme on the HLA-B*27 peptidome may affect other potentially pathogenic features of this molecule, with consequences in the B*27-positive disease.

DATA AVAILABILITY

The mass spectrometry proteomics data have been deposited to the ProteomeXchange Consortium via the PRIDE partner repository (http://www.ebi.ac.uk/pride) with the dataset identifier: PXD014804.

* Supported by grants SAF2017/86578-R (Plan Nacional de I+D+i) to JALC, PI16CIII/00013 (Acción Estratégica de Salud) and S2018/BAA-4480 (Comunidad de Madrid) to PL, Israel Science Foundation, grant N. 1435/16 to AA, and an institutional grant of the Fundación Ramón Areces to the Centro de Biología Molecular *Severo Ochoa.* EL is a recipient of a Juan de la Cierva (FJCI-2016-28335) award from the Government of SPAIN.

S This article contains supplemental material Tables S1 and S2 and Figs. S1–S12.

‖To whom correspondence should be addressed: Unidad de Presentación y Regulación Inmunes, Centro Nacional de Microbiología, Instituto de Salud Carlos III, 28220 Majadahonda, Madrid, Spain. Tel.: 34-91-822 34 19. E-mail: elorente@isciii.es.

Author contributions: E.L. and J.A.L.d.C. designed research; E.L., A.M.-E., E.B., A.A., and J.A.L.d.C. performed research; E.L., J.R.-A., E.B., P.L., and A.A. contributed new reagents/analytic tools; E.L., P.G., E.B., A.A., and J.A.L.d.C. analyzed data; E.L. and J.A.L.d.C. wrote the paper; and A.M.-E. contributed fundamental ideas and discussions for the article.

REFERENCES

1. Saric, T., Chang, S. C., Hattori, A., York, I. A., Markant, S., Rock, K. L., Tsujimoto, M., and Goldberg, A. L. (2002) An IFN-gamma-induced aminopeptidase in the ER, ERAP1, trims precursors to MHC class I-presented peptides. *Nat. Immunol.* **3,** 1169–1176
2. Saveanu, L., Carroll, O., Lindo, V., Del Val, M., Lopez, D., Lepelletier, Y., Greer, F., Schomburg, L., Fruci, D., Niedermann, G., and Van Endert, P. M. (2005) Concerted peptide trimming by human ERAP1 and ERAP2 aminopeptidase complexes in the endoplasmic reticulum. *Nat. Immunol.* **6,** 689–697
3. York, I. A., Chang, S. C., Saric, T., Keys, J. A., Favreau, J. M., Goldberg, A. L., and Rock, K. L. (2002) The ER aminopeptidase ERAP1 enhances or

limits antigen presentation by trimming epitopes to 8–9 residues. *Nat. Immunol.* **3,** 1177–1184
4. López de Castro, J. A., Alvarez-Navarro, C., Brito, A., Guasp, P., Martin-Esteban, A., and Sanz-Bravo, A. (2016) Molecular and pathogenic effects of endoplasmic reticulum aminopeptidases ERAP1 and ERAP2 in MHC-I-associated inflammatory disorders: Towards a unifying view. *Mol. Immunol.* **77,** 193–204
5. Hearn, A., York, I. A., and Rock, K. L. (2009) The specificity of trimming of MHC class I-presented peptides in the endoplasmic reticulum. *J. Immunol.* **183,** 5526–5536
6. Chang, S. C., Momburg, F., Bhutani, N., and Goldberg, A. L. (2005) The ER aminopeptidase, ERAP1, trims precursors to lengths of MHC class I peptides by a "molecular ruler" mechanism. *Proc. Natl. Acad. Sci. U.S.A.* **102,** 17107–17112
7. Mpakali, A., Giastas, P., Mathioudakis, N., Mavridis, I. M., Saridakis, E., and Stratikos, E. (2015) Structural basis for antigenic peptide recognition and processing by ER aminopeptidase 2. *J. Biol. Chem.* **290,** 26021–26032
8. Ombrello, M. J., Kastner, D. L., and Remmers, E. F. (2015) Endoplasmic reticulum-associated amino-peptidase 1 and rheumatic disease: Genetics. *Curr. Opin. Rheumatol.* **27,** 349–356
9. Evnouchidou, I., Birtley, J., Seregin, S., Papakyriakou, A., Zervoudi, E., Samiotaki, M., Panayotou, G., Giastas, P., Petrakis, O., Georgiadis, D., Amalfitano, A., Saridakis, E., Mavridis, I. M., and Stratikos, E. (2012) A common single nucleotide polymorphism in endoplasmic reticulum aminopeptidase 2 induces a specificity switch that leads to altered antigen processing. *J. Immunol.* **189,** 2383–2392
10. Andrés, A. M., Dennis, M. Y., Kretzschmar, W. W., Cannons, J. L., Lee-Lin, S. Q., Hurle, B., Schwartzberg, P. L., Williamson, S. H., Bustamante, C. D., Nielsen, R., Clark, A. G., and Green, E. D. (2010) Balancing selection maintains a form of ERAP2 that undergoes nonsense-mediated decay and affects antigen presentation. *PLoS. Genet.* **6,** e1001157
11. Franke, A., McGovern, D. P., Barrett, J. C., Wang, K., Radford-Smith, G. L., Ahmad, T., Lees, C. W., Balschun, T., Lee, J., Roberts, R., Anderson, C. A., Bis, J. C., Bumpstead, S., Ellinghaus, D., Festen, E. M., Georges, M., Green, T., Haritunians, T., Jostins, L., Latiano, A., Mathew, C. G., Montgomery, G. W., Prescott, N. J., Raychaudhuri, S., Rotter, J. I., Schumm, P., Sharma, Y., Simms, L. A., Taylor, K. D., Whiteman, D., Wijmenga, C., Baldassano, R. N., Barclay, M., Bayless, T. M., Brand, S., Büning, C., Cohen, A., Colombel, J. F., Cottone, M., Stronati, L., Denson, T., De Vos, M., D'Inca, R., Dubinsky, M., Edwards, C., Florin, T., Franchimont, D., Gearry, R., Glas, J., Van Gossum, A., Guthery, S. L., Halfvarson, J., Verspaget, H. W., Hugot, J. P., Karban, A., Laukens, D., Lawrance, I., Lemann, M., Levine, A., Libioulle, C., Louis, E., Mowat, C., Newman, W., Panés, J., Phillips, A., Proctor, D. D., Regueiro, M., Russell, R., Rutgeerts, P., Sanderson, J., Sans, M., Seibold, F., Steinhart, A. H., Stokkers, P. C., Torkvist, L., Kullak-Ublick, G., Wilson, D., Walters, T., Targan, S. R., Brant, S. R., Rioux, J. D., D'Amato, M., Weersma, R. K., Kugathasan, S., Griffiths, A. M., Mansfield, J. C., Vermeire, S., Duerr, R. H., Silverberg, M. S., Satsangi, J., Schreiber, S., Cho, J. H., Annese, V., Hakonarson, H., Daly, M. J., and Parkes, M. (2010) Genome-wide meta-analysis increases to 71 the number of confirmed Crohn's disease susceptibility loci. *Nat. Genet.* **42,** 1118–1125
12. Mahdi, B. M. (2015) Role of HLA typing on Crohn's disease pathogenesis. *Ann. Med. Surg. (London)* **4,** 248–253
13. López de Castro, J. A. (2018) How ERAP1 and ERAP2 Shape the Peptidomes of Disease-Associated MHC-I Proteins. *Front Immunol.* **9,** 2463
14. Cortes, A., Pulit, S. L., Leo, P. J., Pointon, J. J., Robinson, P. C., Weisman, M. H., Ward, M., Gensler, L. S., Zhou, X., Garchon, H. J., Chiocchia, G., Nossent, J., Lie, B. A., Førre, Ø., Tuomilehto, J., Laiho, K., Bradbury, L. A., Elewaut, D., Burgos-Vargas, R., Stebbings, S., Appleton, L., Farrah, C., Lau, J., Haroon, N., Mulero, J., Blanco, F. J., Gonzalez-Gay, M. A., Lopez-Larrea, C., Bowness, P., Gaffney, K., Gaston, H., Gladman, D. D., Rahman, P., Maksymowych, W. P., Crusius, J. B., van der Horst-Bruinsma, I. E., Valle-Oñate, R., Romero-Sanchez, C., Hansen, I. M., Pimentel-Santos, F. M., Inman, R. D., Martin, J., Breban, M., Wordsworth, B. P., Reveille, J. D., Evans, D. M., de Bakker, P. I., and Brown, M. A. (2015) Major histocompatibility complex associations of ankylosing spondylitis are complex and involve further epistasis with ERAP1. *Nat. Commun.* **6,** 7146
15. Cortes, A., Hadler, J., Pointon, J. P., Robinson, P. C., Karaderi, T., Leo, P., Cremin, K., Pryce, K., Harris, J., Lee, S., Joo, K. B., Shim, S. C., Weisman, M., Ward, M., Zhou, X., Garchon, H. J., Chiocchia, G., Nossent, J., Lie, B. A., Førre, Ø., Tuomilehto, J., Laiho, K., Jiang, L., Liu, Y., Wu, X., Bradbury, L. A., Elewaut, D., Burgos-Vargas, R., Stebbings, S., Appleton, L., Farrah, C., Lau, J., Kenna, T. J., Haroon, N., Ferreira, M. A., Yang, J., Mulero, J., Fernandez-Sueiro, J. L., Gonzalez-Gay, M. A., Lopez-Larrea, C., Deloukas, P., Donnelly, P., Bowness, P., Gafney, K., Gaston, H., Gladman, D. D., Rahman, P., Maksymowych, W. P., Xu, H., Crusius, J. B., van der Horst-Bruinsma, I. E., Chou, C. T., Valle-Onate, R., Romero-Sanchez, C., Hansen, I. M., Pimentel-Santos, F. M., Inman, R. D., Videm, V., Martin, J., Breban, M., Reveille, J. D., Evans, D. M., Kim, T. H., Wordsworth, B. P., and Brown, M. A. (2013) Identification of multiple risk variants for ankylosing spondylitis through high-density genotyping of immune-related loci. *Nat. Genet.* **45,** 730–738
16. Robinson, P. C., Costello, M. E., Leo, P., Bradbury, L. A., Hollis, K., Cortes, A., Lee, S., Joo, K. B., Shim, S. C., Weisman, M., Ward, M., Zhou, X., Garchon, H. J., Chiocchia, G., Nossent, J., Lie, B. A., Førre, Ø., Tuomilehto, J., Laiho, K., Jiang, L., Liu, Y., Wu, X., Elewaut, D., Burgos-Vargas, R., Gensler, L. S., Stebbings, S., Haroon, N., Mulero, J., Fernandez-Sueiro, J. L., Gonzalez-Gay, M. A., Lopez-Larrea, C., Bowness, P., Gafney, K., Gaston, J. S., Gladman, D. D., Rahman, P., Maksymowych, W. P., Xu, H., van der Horst-Bruinsma, I. E., Chou, C. T., Valle-Onate, R., Romero-Sanchez, M. C., Hansen, I. M., Pimentel-Santos, F. M., Inman, R. D., Martin, J., Breban, M., Evans, D., Reveille, J. D., Kim, T. H., Wordsworth, B. P., and Brown, M. A. (2015) ERAP2 is associated with ankylosing spondylitis in HLA-B27-positive and HLA-B27-negative patients. *Ann. Rheum. Dis.* **74,** 1627–1629
17. Martin-Esteban, A., Guasp, P., Barnea, E., Admon, A., and López de Castro, J. A. (2016) Functional interaction of the ankylosing spondylitis associated endoplasmic reticulum aminopeptidase 2 with the HLA-B*27 peptidome in human cells. *Arthritis Rheumatol.* **68,** 2466–2475
18. Martin-Esteban, A., Sanz-Bravo, A., Guasp, P., Barnea, E., Admon, A., and López de Castro, J. A. (2017) Separate effects of the ankylosing spondylitis associated ERAP1 and ERAP2 aminopeptidases determine the influence of their combined phenotype on the HLA-B*27 peptidome. *J. Autoimmun.* **79,** 28–38
19. Sanz-Bravo, A., Martín-Esteban, A., Kuiper, J. J. W., García-Peydró, M., Barnea, E., Admon, A., and Lopez de Castro, J. A. (2018) Allele-specific alterations in the peptidome underlie the joint association of HLA-A*29:02 and endoplasmic reticulum aminopeptidase 2 (ERAP2) with birdshot chorioretinopathy. *Mol. Cell Proteomics* **17,** 1564–1577
20. Guasp, P., Lorente, E., Martin-Esteban, A., Barnea, E., Romania, P., Fruci, D., Kuiper, J. J. W., Admon, A., and Lopez de Castro, J. A. (2019) Redundancy and complementarity between ERAP1 and ERAP2 revealed by their effects on the Behcet's disease-associated HLA-B*51 peptidome. *Mol. Cell. Proteomics* **18,** 1491–1510
21. Marcilla, M., Alpízar, A., Lombardía, M., Ramos-Fernandez, A., Ramos, M., and Albar, J. P. (2014) Increased diversity of the HLA-B40 ligandome by the presentation of peptides phosphorylated at their main anchor residue. *Mol. Cell. Proteomics* **13,** 462–474
22. Ben Dror, L., Barnea, E., Beer, I., Mann, M., and Admon, A. (2010) The HLA-B*2705 peptidome. *Arthritis Rheum.* **62,** 420–429
23. Jardetzky, T. S., Lane, W. S., Robinson, R. A., Madden, D. R., and Wiley, D. C. (1991) Identification of self peptides bound to purified HLA-B27. *Nature* **353,** 326–329
24. Lopez de Castro, J. A., Alvarez, I., Marcilla, M., Paradela, A., Ramos, M., Sesma, L., and Vázquez, M. (2004) HLA-B27: A registry of constitutive peptide ligands. *Tissue Antigens* **63,** 424–445
25. Zemmour, J., Little, A. M., Schendel, D. J., and Parham, P. (1992) The HLA-A,B "negative" mutant cell line C1R expresses a novel HLA-B35 allele, which also has a point mutation in the translation initiation codon. *J. Immunol.* **148,** 1941–1948
26. García-Medel, N., Sanz-Bravo, A., Van Nguyen, D., Galocha, B., Gómez-Molina, P., Martin-Esteban, A., Alvarez-Navarro, C., and López de Castro, J. A. (2012) Functional interaction of the ankylosing spondylitis-associated endoplasmic reticulum aminopeptidase 1 polymorphism and HLA-B27 in vivo. *Mol. Cell Proteomics.* **11,** 1416–1429
27. Barnstable, C. J., Bodmer, W. F., Brown, G., Galfre, G., Milstein, C., Williams, A. F., and Ziegler, A. (1978) Production of monoclonal antibodies to group A erythrocytes, HLA and other human cell surface antigens. New tools for genetic analysis. *Cell* **14,** 9–20
28. Guasp, P., Alvarez-Navarro, C., Gomez-Molina, P., Martín-Esteban, A., Marcilla, M., Barnea, E., Admon, A., and López de Castro, J. A. (2016)

The peptidome of the Behcet's disease-associated HLA-B*51:01 includes two sub-peptidomes differentially shaped by ERAP1. *Arthritis Rheumatol.* **68,** 505–515
29. Ishihama, Y., Rappsilber, J., Andersen, J. S., and Mann, M. (2002) Microcolumns with self-assembled particle frits for proteomics. *J. Chromatogr. A* **979,** 233–239
30. Karosiene, E., Lundegaard, C., Lund, O., and Nielsen, M. (2012) NetMHCcons: a consensus method for the major histocompatibility complex class I predictions. *Immunogenetics* **64,** 177–186
31. Kyte, J., and Doolittle, R. F. (1982) A simple method for displaying the hydropathic character of a protein. *J. Mol. Biol.* **157,** 105–132
32. Cox, J., and Mann, M. (2008) MaxQuant enables high peptide identification rates, individualized p.p.b.-range mass accuracies and proteome-wide protein quantification. *Nat. Biotechnol.* **26,** 1367–1372
33. Cox, J., Neuhauser, N., Michalski, A., Scheltema, R. A., Olsen, J. V., and Mann, M. (2011) Andromeda: A peptide search engine integrated into the MaxQuant environment. *J. Proteome. Res.* **10,** 1794–1805
34. Schittenhelm, R. B., Dudek, N. L., Croft, N. P., Ramarathinam, S. H., and Purcell, A. W. (2014) A comprehensive analysis of constitutive naturally processed and presented HLA-C*04:01 (Cw4)-specific peptides. *Tissue Antigens* **83,** 174–179
35. Martín-Esteban, A., Gómez-Molina, P., Sanz-Bravo, A., and López de Castro, J. A. (2014) Combined effects of ankylosing spondylitis-associated ERAP1 polymorphisms outside the catalytic and peptide-binding sites on the processing of natural HLA-B27 ligands. *J. Biol. Chem.* **289,** 3978–3990
36. Herberts, C. A., Neijssen, J. J., de Haan, J., Janssen, L., Drijfhout, J. W., Reits, E. A., and Neefjes, J. J. (2006) Cutting edge: HLA-B27 acquires many N-terminal dibasic peptides: Coupling cytosolic peptide stability to antigen presentation. *J. Immunol.* **176,** 2697–2701
37. Benjamin, R., and Parham, P. (1990) Guilt by association: HLA-B27 and ankylosing spondylitis. *Immunol. Today* **11,** 137–142
38. Colbert, R. A., Tran, T. M., and Layh-Schmitt, G. (2014) HLA-B27 misfolding and ankylosing spondylitis. *Mol. Immunol.* **57,** 44–51
39. Allen, R. L., O'Callaghan, C. A., McMichael, A. J., and Bowness, P. (1999) Cutting edge: HLA-B27 can form a novel β2-microglobulin-free heavy chain homodimer structure. *J. Immunol.* **162,** 5045–5048
40. Bowness, P., Ridley, A., Shaw, J., Chan, A. T., Wong-Baeza, I., Fleming, M., Cummings, F., McMichael, A., and Kollnberger, S. (2011) Th17 cells expressing KIR3DL2+ and responsive to HLA-B27 homodimers are increased in ankylosing spondylitis. *J. Immunol.* **186,** 2672–2680